

# A Molecular gas rich GRB host galaxy at the peak of cosmic star formation

M. Arabsalmani<sup>1,2,3\*</sup>, E. Le Floc’h<sup>1,2</sup>, H. Dannerbauer<sup>4,5</sup>, C. Feruglio<sup>6</sup>, E. Daddi<sup>1,2</sup>,  
L. Ciesla<sup>1,2</sup>, V. Charmandaris<sup>7,8</sup>, J. Japelj<sup>9</sup>, S. D. Vergani<sup>3</sup>, P.-A. Duc<sup>10,1,2</sup>, S. Basa<sup>11</sup>,  
F. Bournaud<sup>1,2</sup>, D. Elbaz<sup>1,2</sup>

<sup>1</sup> IRFU, CEA, Université Paris-Saclay, F-91191 Gif-sur-Yvette, France

<sup>2</sup> Université Paris Diderot, AIM, Sorbonne Paris Cité, CEA, CNRS, F-91191 Gif-sur-Yvette, France

<sup>3</sup> GEPI, Observatoire de Paris, PSL Research University, CNRS, Place Jules Janssen, 92190 Meudon, France

<sup>4</sup> Instituto de Astrofísica de Canarias (IAC), E-38205 La Laguna, Tenerife, Spain

<sup>5</sup> Universidad de La Laguna, Dpto. Astrofísica, E-38206 La Laguna, Tenerife, Spain

<sup>6</sup> INAF Osservatorio Astronomico di Trieste, Via G. Tiepolo 11, I-34124 Trieste

<sup>7</sup> Institute for Astronomy, Astrophysics, Space Applications & Remote Sensing, National Observatory of Athens, GR-15236, Penteli, Greece

<sup>8</sup> Department of Physics, University of Crete, GR-71003 Heraklion, Greece

<sup>9</sup> Anton Pannekoek Institute for Astronomy, University of Amsterdam, Science Park 904, 1098 XH Amsterdam, The Netherlands

<sup>10</sup> Université de Strasbourg, CNRS, Observatoire astronomique de Strasbourg, UMR 7550, F-67000 Strasbourg, France

<sup>11</sup> LAM - Laboratoire d’Astrophysique de Marseille, 13388 Marseille Cedex 13, France

## ABSTRACT

We report the detection of the CO(3-2) emission line from the host galaxy of Gamma Ray Burst (GRB) 080207 at  $z = 2.086$ . This is the first detection of molecular gas in emission from a GRB host galaxy beyond redshift 1. We find this galaxy to be rich in molecular gas with a mass of  $1.1 \times 10^{11} M_{\odot}$  assuming  $\alpha_{\text{CO}} = 4.36 M_{\odot} (\text{K km s}^{-1} \text{pc}^2)^{-1}$ . The molecular gas mass fraction of the galaxy is  $\sim 0.5$ , typical of star forming galaxies (SFGs) with similar stellar masses and redshifts. With a  $\text{SFR}_{\text{FIR}}$  of  $260 M_{\odot} \text{yr}^{-1}$ , we measure a molecular-gas-depletion timescale of 0.43 Gyr, near the peak of the depletion timescale distribution of SFGs at similar redshifts. Our findings are therefore in contradiction with the proposed molecular gas deficiency in GRB host galaxies. We argue that the reported molecular gas deficiency for GRB hosts could be the artifact of improper comparisons or neglecting the effect of the typical low metallicities of GRB hosts on the CO-to-molecular-gas conversion factor. We also compare the kinematics of the CO(3-2) emission line to that of the  $\text{H}\alpha$  emission line from the host galaxy. We find the  $\text{H}\alpha$  emission to have contributions from two separate components, a narrow and a broad one. The narrow component matches the CO emission well in velocity space. The broad component, with a FWHM of  $\sim 1100 \text{ km s}^{-1}$ , is separated by  $+390 \text{ km s}^{-1}$  in velocity space from the narrow component. We speculate this broad component to be associated with a powerful outflow in the host galaxy or in an interacting system.

**Key words:** gamma-ray burst: general – galaxies: high-redshift – galaxies: star formation – galaxies: kinematics and dynamics – submillimetre: galaxies

## 1 INTRODUCTION

Long-duration Gamma Ray Bursts (GRBs) are believed to originate in massive stars and hence are beacons of star-forming galaxies (e.g. Sokolov et al. 2001; Le Floc’h et al. 2003; Fruchter et al. 2006). The detectability of these extremely bright and dust-

penetrating explosions is independent of the brightness and dust content of their host galaxies. Hence they provide a unique method for sampling star-forming galaxies throughout the Universe without a luminosity bias, a challenge that significantly impacts even the deepest flux-limited galaxy surveys. GRB host galaxies typically show very high HI column densities ( $N(\text{HI}) > 10^{21} \text{ cm}^{-2}$ ) measured through the Lyman- $\alpha$  absorption line in GRBs spectra (e.g., Jakobsson et al. 2006; Prochaska et al. 2007; Fynbo et al. 2009).

\* E-mail: maryam.arabsalmani@cea.fr

Contrarily, molecular gas in absorption has been detected in the spectra of only four GRBs (Prochaska et al. 2009; Krühler et al. 2013; D’Elia et al. 2014; Friis et al. 2015). Dissociation by GRB emission radiation is ruled out as the cause of the apparent low detection rate of molecular gas in GRB afterglows given the large distances between GRB locations and gas detected in absorption (larger than several hundreds of pc, see Ledoux et al. 2009). Studies of absorbing systems in lines of sight towards quasars show that the detection of molecular gas is not coupled to the high  $N(\text{H I})$ , but rather to high metallicities and depletion factors which increases the formation rate of  $\text{H}_2$  onto dust grains (see Noterdaeme et al. 2008). This is consistent with the low detection rate of molecular lines in GRB afterglows (Ledoux et al. 2009; Krühler et al. 2013) as GRB host galaxies typically have low metallicities (e.g. Savaglio et al. 2009; Fynbo et al. 2009).

Detection of molecular gas in emission has been reported for three GRB host galaxies at redshifts  $z = 0.0087, 0.089, \text{ and } 0.81$  (Hatsukade et al. 2014; Stanway et al. 2015b; Michałowski et al. 2016; see also Perley et al. 2017b). All three hosts are reported to be deficient in molecular gas (with respect to their stellar masses or star-formation rates), with short molecular-gas-depletion times. This is proposed to be characteristic of the GRB population, suggesting formation of GRBs toward the end of the star formation episodes of their host galaxies (see Stanway et al. 2015b). Intense star-formation in the GRB environment (Hatsukade et al. 2014) as well as formation of stars from atomic gas before its conversion to molecular gas (Michałowski et al. 2016) are alternative hypotheses proposed to explain the apparent tendency of GRB hosts to be deficient in molecular gas.

In this paper we present the properties of molecular gas in the host galaxy of GRB 080207 at  $z = 2.086$  through the observations performed with the Plateau de Bure / Northern Extended Millimeter Array (NOEMA) at 112 GHz and also with the Large Apex Bolometer Camera (LABOCA) on the Atacama Pathfinder Experiment (APEX) at  $870 \mu\text{m}$ <sup>1</sup>. The host galaxy of GRB 080207 is a massive, extremely red and dusty star-forming galaxy (Hunt et al. 2011; Rossi et al. 2012), making it a promising candidate for detection of molecular gas emission lines. The redshift of the galaxy being at the peak of the cosmic star-formation makes it even more interesting for studies of molecular gas, the fuel of star formation. The observations and data reduction are described in Section 2. Our findings and results are presented in Section 3. In Section 4 we discuss the reported molecular gas deficiency in GRB host galaxies, and finally in Section 5 we present a summary. Throughout this paper we use a flat  $\Lambda\text{CDM}$  with  $H_0=69.6 \text{ km s}^{-1} \text{ Mpc}^{-1}$  and  $\Omega_m=0.286$ .

## 2 OBSERVATIONS AND DATA REDUCTION

We targeted the host galaxy of GRB 080207 for the CO(3-2) transition with Plateau de Bure / NOEMA in C-configuration (project code w0c9) in May 2013 using a bandwidth of 2.3 GHz, centred at the red-shifted CO(3-2) line frequency of 112.06 GHz. The observations were performed with the dual polarization mode and with a total on-source time of 9.12 hours. Data were reduced and analyzed with the Grenoble Image and Line Data Analysis Software. After flagging and calibration process, the calibrated visibilities were mapped to produce a spectral cube assuming natural

<sup>1</sup> Based on observations made with ESO telescopes at the La Silla Paranal Observatory under programme ID 089.F-9304.

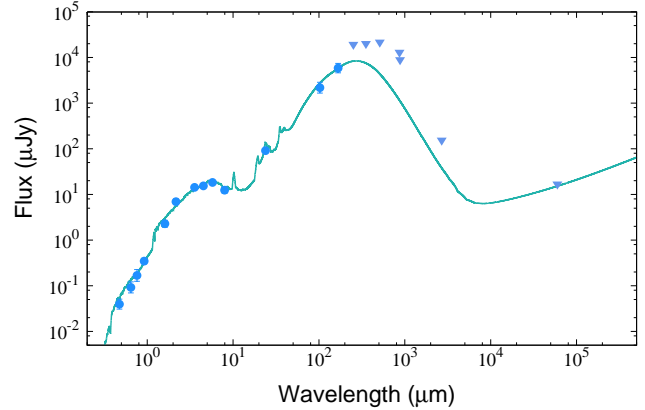


**Figure 1.** The best-fitting Spectral Energy Distribution (SED) for the host galaxy of GRB 080207 obtained using *LePhare*. The x-axis is wavelength in the observer frame. The circles present the photometry values of the GRB host while the triangles show the upper limit photometries.

weighting, reaching a rms-noise of 0.7 mJy/beam in line-free channels with 50 MHz width and a synthesized beam of  $5.1'' \times 4.5''$ . For the continuum of the galaxy we reached a  $3\sigma$  upper limit of 0.16 mJy/beam, without detecting the galaxy.

We also observed this host at  $870 \mu\text{m}$  with the bolometer camera LABOCA (Siringo et al. 2009) on the APEX telescope (program ID 089.F-9304). The observations were carried out in April and August 2012 in service mode with typical pwvs between 0.5–1.8 mm. We observed our target in point source photometry mode (where the target is placed on a reference pixel) for a total observing time of 4.2 hours. Data reduction was performed with the CRUSH software (Kovács 2008), which led to a non-detection with a  $3\sigma$  upper limit flux of 9.0 mJy for the galaxy at  $870 \mu\text{m}$ .

## 3 RESULTS

### 3.1 Modeling the Spectral Energy Distribution of the host

The host galaxy of GRB 080207 is a massive galaxy with a stellar mass reported in a range of  $10^{11.05} - 10^{11.17} M_{\odot}$  (Hunt et al. 2011, 2014; Svensson et al. 2012; Perley et al. 2013). The reported star formation rate (SFR) of the galaxy varies in a large range of  $46 - 416 M_{\odot} \text{ yr}^{-1}$ , measured from different methods (Svensson et al. 2012; Krühler et al. 2012; Hunt et al. 2014; Perley et al. 2013). Considering that this galaxy is extremely red and dusty, its far-Infrared luminosity ( $L_{\text{FIR}}$ ) will provide the best estimate for its SFR.

We add the two upper limits from our observations with APEX and Plateau de Bure / NOEMA to all available photometry from UV up to radio (Hunt et al. 2011; Perley et al. 2013; Hunt et al. 2014) and use *LePhare* (Arnouts et al. 1999) to model the Spectral Energy Distribution (SED) of the host galaxy. We use the radio band photometry of the galaxy at 5.2 GHz from Perley et al. (2013) as an upper limit in our SED modeling since the reported value could have contamination from the radio-afterglow of the GRB itself (see Perley et al. 2013, for details on the radio photometry of the host, also see Perley et al. 2017a, for examples of the radio afterglow contamination several years after GRB events).

For modeling the stellar emission from the host galaxy, we use the Stellar Population Synthesis templates developed by

**Table 1.** The properties of GRB 080207 host galaxy obtained from SED modeling. We use the calibration from Kennicutt & Evans (2012) in order to obtain the  $\text{SFR}_{\text{FIR}}$  from  $L_{\text{FIR}}$ .

$M_*$ ( $M_\odot$ )	$E(B-V)$	$\log(L_{\text{FIR}}/L_\odot)$	$\text{SFR}_{\text{FIR}}$ ( $M_\odot \text{ yr}^{-1}$ )
$(9.1_{-2.2}^{+1.4}) \times 10^{10}$	0.5	$12.18_{-0.10}^{+0.06}$	$260_{-53}^{+39}$

Bruzual & Charlot (2003). We limit our models to the BC03–m62 library – the templates with solar metallicity since the measured metallicity for GRB 080207 host galaxy is  $1.1 Z_\odot$  (Krühler et al. 2015). We use the Chabrier IMF (Chabrier 2003) and consider both the exponentially declining star formation history ( $\text{SFR} \propto e^{-t/\tau}$ ) with  $\tau$  values of 0.1, 0.3, 1, 2, 3, 5, 10, 15, and 30 Gyr, as well as the delayed star formation history ( $\text{SFR} \propto -te^{t/\tau}$ ). The dust extinction law from Calzetti et al. (2000) is applied to the templates with  $E(B-V)$  values ranging between 0.0 and 1.2 with a step size of 0.1. Using *LePhare* we separately model the SED of the galaxy in infrared-radio wavelengths with templates from Chary & Elbaz (2001).

The best-fitting SED model for the host galaxy is presented in Fig. 1. Estimated galaxy properties based on the SED modeling are provided in Table 1. We use the calibration from Kennicutt & Evans (2012) and estimate the  $\text{SFR}_{\text{FIR}}$  of the galaxy to be  $260_{-53}^{+39} M_\odot \text{ yr}^{-1}$  from the measured FIR luminosity of  $\log(L_{\text{FIR}}/L_\odot) = 12.18_{-0.10}^{+0.06}$ . Our stellar mass measurement is consistent with the values obtained by previous studies (Hunt et al. 2011, 2014; Svensson et al. 2012; Perley et al. 2013). The host galaxy of GRB 080207 happens to be a main-sequence star-forming galaxy (Elbaz et al. 2011). It also follows the mass-metallicity relation of the general star-forming galaxy population with similar redshifts (see Arabsalmani et al. 2018).

### 3.2 Molecular gas properties of the host

We detect the CO(3-2) emission line from the host galaxy of GRB 080207 with a  $7\sigma$  significance (all the measurements for the molecular gas properties of the GRB host are listed in Table 2). Fig. 2 shows the velocity-integrated CO(3-2) map (in contours) overlaid on the *Hubble Space Telescope* (*HST*) image of the host galaxy (with the WFC3/F110W filter, centred at  $11534.459 \text{ \AA}$ ).

As the source is spatially unresolved, we use the fluxes from the beam centred on the source position only. The CO(3-2) line flux in the velocity space (relative to  $z = 2.0857$ ) is shown in Fig. 3. From the Gaussian fit to the CO line, we measure a redshift of  $z = 2.0857 \pm 0.0002$ , consistent with the redshift of  $z = 2.0858 \pm 0.0003$  derived from the nebular emission lines in the host spectrum by Krühler et al. (2012). We measure a velocity-integrated flux density of  $0.63 \pm 0.08 \text{ Jy km s}^{-1}$  over five channels covering a velocity spread of  $267 \text{ km s}^{-1}$ . This leads to a brightness temperature luminosity, as defined in Obreschkow et al. (2009), of  $L_{\text{CO}(3-2)}^{\text{T}} = (1.54 \pm 0.20) \times 10^{10} \text{ K km s}^{-1} \text{ pc}^2$ , where

$$L^{\text{T}} (\text{K km s}^{-1} \text{ pc}^2) = 3.255 \times 10^7 (\nu_{\text{line,obs}} (\text{GHz}))^{-2} \times (D_L (\text{Mpc}))^2 (1+z)^{-3} (S\Delta v (\text{Jy km s}^{-1})),$$

same as the  $L'$  defined in Solomon et al. (1997). From the best-fitting Gaussian we obtain a full-width-at-half-maximum (FWHM) of  $191 \pm 35 \text{ km s}^{-1}$  for the CO(3-2) line.

The left panel of Fig. 4 shows the  $\text{SFR}-L_{\text{CO}(3-2)}^{\text{T}}$  correla-

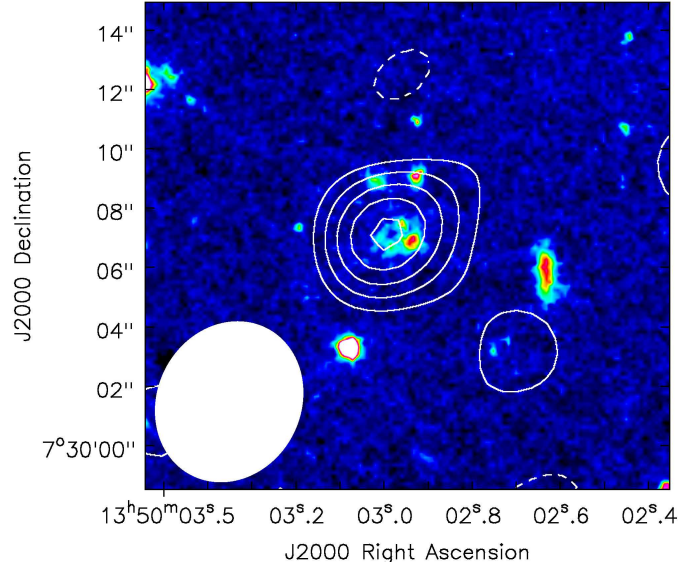


**Figure 2.** The velocity-integrated CO(3-2) map (in contours) overlaid on the *HST* image of the host galaxy. The beam-size is  $4.8'' \times 5.5''$ . The outermost contour is at  $2\sigma$  significance, with subsequent contours in steps of  $1\sigma$ . The negative contours are at  $-2\sigma$  level.

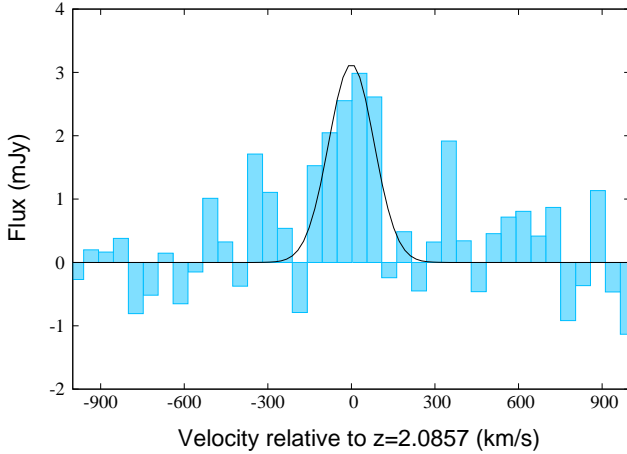
tion for star-forming galaxies (SFGs) with the position of GRB 080207 host galaxy marked with a black circle. Our target host clearly falls on the same region as typical SFGs with similar redshifts. Although the SFR of our target galaxy happens to be on the higher side given its stellar mass, it places the galaxy amongst the main-sequence star-forming galaxies (see Fig. 1 of Rodighiero et al. 2011). Therefore, in order to convert the measured  $L_{\text{CO}(3-2)}^{\text{T}}$  to a brightness temperature luminosity of CO(1-0) we use a  $R_{31} = L_{\text{CO}(3-2)}^{\text{T}}/L_{\text{CO}(1-0)}^{\text{T}}$  of 0.6 from Carilli & Walter (2013) which is the value for main-sequence star-forming galaxies (see also Dannerbauer et al. 2009; Daddi et al. 2015) and obtain  $L_{\text{CO}(1-0)}^{\text{T}} = 2.56 \times 10^{10} \text{ K km s}^{-1} \text{ pc}^2$ .

To estimate the molecular gas mass for the host galaxy we need to assume a reasonable CO-to-molecular-gas conversion factor ( $\alpha_{\text{CO}}$ ). The GRB host has a  $12+\log[\text{O}/\text{H}]$  of 8.7 (Krühler et al. 2015), equivalent to a metallicity of 1.1 solar. Using the Galactic  $\alpha_{\text{CO}}$  of  $4.36 M_\odot (\text{K km s}^{-1} \text{ pc}^2)^{-1}$ , we estimate a molecular gas mass of  $1.1 \times 10^{11} M_\odot$ . With a stellar mass of  $9.1 \times 10^{10} M_\odot$  (see Table. 1), we find the molecular gas fraction of the host to be  $f_{\text{mol-gas}} \sim 0.5$ , where  $f_{\text{mol-gas}}$  is  $M_{\text{mol-gas}}/(M_{\text{mol-gas}} + M_*)$ . This molecular gas fraction is typical of SFGs with similar stellar masses and redshifts (see Fig. 6 of Tacconi et al. 2013, for the gas fractions of star forming galaxies at  $z = 1 - 3$ ). We also find a molecular-gas-depletion timescale ( $M_{\text{mol}}/\text{SFR}$ ) of 0.43 Gyr for the GRB host which is at the peak of the depletion timescale distribution of SFGs at similar redshifts (see Fig. 7 of Tacconi et al. 2013).

We use the half-light-radius of  $R_{0.5} = 3.4 \text{ kpc}$  (from Svensson et al. 2012, remeasured and confirmed by us) and calculate a SFR surface-density of  $\Sigma_{\text{SFR}} = 3.6 M_\odot \text{ yr}^{-1} \text{ kpc}^{-2}$  and a molecular gas surface-density of  $\Sigma_{\text{mol-gas}} = 1.5 \times 10^3 M_\odot \text{ pc}^{-2}$  for the host. The right panel of Fig. 4 shows the Kennicutt-Schmidt (K-S) relation (Kennicutt 1998) with a black circle representing the GRB host. The host galaxy of GRB 080207 clearly follows the K-S relation of the SFGs.

**Table 2.** The molecular gas properties of GRB 080207 host galaxy.

Redshift	$\text{FWHM}_{\text{CO}(3-2)}$ ( $\text{km s}^{-1}$ )	$(S\Delta v)_{\text{CO}(3-2)}$ ( $\text{Jy km s}^{-1}$ )	$L_{\text{CO}(3-2)}^T$ ( $\text{K km s}^{-1} \text{pc}^2$ )	$M_{\text{mol-gas}}$ ( $M_{\odot}$ )	$\Sigma_{\text{SFR}}$ ( $M_{\odot} \text{yr}^{-1} \text{kpc}^{-2}$ )	$\Sigma_{\text{mol-gas}}$ ( $M_{\odot} \text{pc}^{-2}$ )
2.086	$191 \pm 35$	$0.63 \pm 0.08$	$(1.54 \pm 0.20) \times 10^{10}$	$1.1 \times 10^{11}$	3.6	$1.5 \times 10^3$

**Figure 3.** The CO(3-2) emission line from the host galaxy of GRB 080207 detected by Plateau de Bure / NOEMA with a channel-width of  $53 \text{ km s}^{-1}$ . The best-fitting Gaussian to the line is shown with a black line.

### 3.3 Kinematics of molecular versus ionized gas

In this section we compare the kinematics of the molecular gas with that of the ionized gas through a comparison between the structure and velocity widths of CO(3-2) and the bright nebular emission lines from the galaxy. For this we use the 1-D extracted VLT/X-shooter spectrum of the host galaxy presented in Krühler et al. (2015) and available at VizieR database (see Krühler et al. 2012, 2015, for the details of the data reduction). A part of the NIR spectrum, covering the wavelengths of  $\text{H}\alpha$  and  $[\text{NII}]6548,6584$  emission lines, is shown in Fig. 5. The  $\text{H}\alpha$  emission line seems to have an extension in the red side, spreading over several hundreds of  $\text{km s}^{-1}$ . This is clearly apparent in the 2-D spectrum of the  $\text{H}\alpha$  line presented in Fig. 3 of Krühler et al. (2012). Although the overall S/N ratio of the X-shooter NIR spectrum of the host is not high, the extension spreading over the velocity range between 350 and 600  $\text{km s}^{-1}$  relative to the redshift of the host, is detected with  $10\sigma$  significance. While the CO(3-2) emission line has a FWHM of  $191 \pm 35 \text{ km s}^{-1}$ , a single Gaussian fit to the  $\text{H}\alpha$  line results in a FWHM of  $790 \pm 60 \text{ km s}^{-1}$ . This is an evidence for the significant contribution from a broad emission in  $\text{H}\alpha$  which is not present in the CO(3-2) emission line.

To investigate this further, we model the galaxy spectrum (shown in Fig. 5) by a two component system. We simultaneously fit double-Gaussian functions (summation of two independent Gaussians) to each of the  $\text{H}\alpha$  and  $[\text{NII}]6548,6584$  lines. We allow the velocity widths of the two components to vary, but for each component set the line-broadening of the  $\text{H}\alpha$  and  $[\text{NII}]$  lines to be the same. The peak fluxes of the  $\text{H}\alpha$  and  $[\text{NII}]6584$  lined associated with the two components are free to vary, but we fix the  $[\text{NII}]6584/[\text{NII}]6564$  ratio to the theoretical value of 2.92 (Acker et al. 1989; Storey & Zeippen 2000) for both components. We therefore have eight free parameters: the  $\text{H}\alpha$  line centres and

broadenings associated with the two components (four parameters), and the peak fluxes of the  $\text{H}\alpha$  and  $[\text{NII}]6584$  lines for the two components (four parameters).

We find the best-fitting model (with a reduced  $\chi^2$  of 1.2) to be the combination of a narrow and a broad component. The narrow component (detected at  $\sim 5\sigma$  significance) is centred at a velocity of  $-67 \pm 13 \text{ km s}^{-1}$  relative to the redshift obtained from the CO(3-2) emission line ( $z = 2.0857$ ), or equivalently, is centred at the redshift of  $2.0850 \pm 0.0001$ . It has a FWHM of  $207 \pm 35 \text{ km s}^{-1}$  (corrected for the typical spectral resolution of  $50 \text{ km s}^{-1}$  in the NIR arm of X-shooter, see Arabsalmani et al. 2015a), consistent with the FWHM of the CO(3-2) emission line. As shown in Fig. 5, the narrow component very well matches the CO(3-2) emission line in velocity space. Note that the peak flux of the CO(3-2) line in Fig. 5 is scaled to match the peak flux of the narrow component of the  $\text{H}\alpha$  emission.

The second component, centred at  $320 \pm 110 \text{ km s}^{-1}$  relative to  $z = 2.0857$ , and detected at  $\sim 3\sigma$  significance, is quite broad with a FWHM of  $1160 \pm 330 \text{ km s}^{-1}$ . The large FWHM of this component is consistent with the signature of a powerful outflow (see Newman et al. 2012a,b). Note that outflows are not necessarily symmetric and depending on their orientation they can be detected as red-shifted or blue-shifted components (see Feruglio et al. 2015, for an example of red-shifted outflowing gas). The broad component accounts for  $77\% \pm 30\%$  of the total  $\text{H}\alpha$  flux. This is similar to the case of an individual clump in the  $z \sim 2$  clumpy SFG presented in Newman et al. (2012a), where the  $\text{H}\alpha$  emission from the clump is dominated by a broad component associated with a strong outflowing gas.

For both components the  $[\text{NII}]6584/\text{H}\alpha$  ratio is roughly 0.2-0.3, which is typical for star-formation-driven outflows, and less than the ratios expected for Active galactic nucleus (AGN) driven outflows (Newman et al. 2012a,b; Förster Schreiber et al. 2014). In addition, the large offset between the two components is against the presence of an AGN being responsible for the broad emission (see Genzel et al. 2014). The low S/N of the NIR spectrum does not allow performing a detailed analysis for the  $\text{H}\beta$  and oxygen lines in order to further investigate the possible contribution from an AGN. We should mention that our SED modeling presented in section 3.1 does not favor the presence of an AGN. Also note that GRB host galaxies typically have high SFR surface-densities (Kelly et al. 2014) which predicts strong star-formation driven outflows from their compact star-forming regions (see Lagos et al. 2013; Arabsalmani et al. 2018).

The presence of a broad component in the  $\text{H}\alpha$  emission line is not uncommon in SFGs at  $z \sim 2$  (Newman et al. 2012a,b; Förster Schreiber et al. 2014; Genzel et al. 2014). It is notable though that in the SFG sample of Genzel et al. (2014) the average flux ratio of the broad to narrow component is  $\sim 0.4$  while for the host of GRB 080207 this ratio is  $\sim 3.4$ . This is also larger than the broad to narrow flux ratios in all the SFGs presented in Newman et al. (2012b, see their Fig.2). The characteristics of the  $\text{H}\alpha$  emission line from the host galaxy of GRB 080207 is more

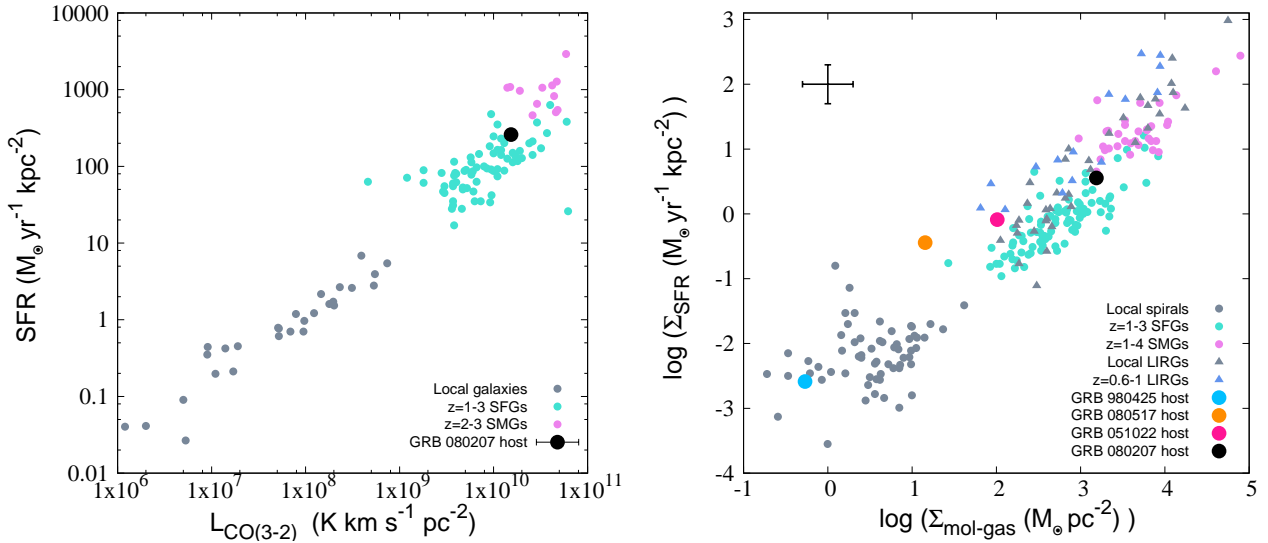


**Figure 4.** *Left panel:* Observed  $L_{\text{CO}(3-2)}^{\text{T}}$  versus SFR, for local Star-Forming Galaxies (SFGs, in gray, from Wilson et al. 2012),  $z = 1 - 3$  SFGs (in green, from Tacconi et al. 2010, 2013), and  $z = 2 - 3$  luminous Sub-Millimetre Galaxies (SMGs, in violet, from Bothwell et al. 2013). The  $L_{\text{CO}(3-2)}^{\text{T}}$  for GRB 080207 host (this work) is marked with a black circle. *Right panel:* Kennicutt-Schmidt relation, for local spiral galaxies (gray circles, from Kennicutt 1998), local Luminous Infrared Galaxies (LIRGs, gray triangles, from Kennicutt 1998),  $z = 0.6 - 1$  LIRGs (blue triangles, from Combes et al. 2013),  $z = 1 - 3$  SFGs (cyan circles, from Daddi et al. 2010; Genzel et al. 2010; Tacconi et al. 2010, 2013), and  $z = 1 - 4$  SMGs (violet circles, from Genzel et al. 2010; Bothwell et al. 2013). Note that for all the sample galaxies the molecular gas mass includes both the  $\text{H}_2$  and  $\text{He}$  mass (with  $M_{\text{He}} = 0.36M_{\text{H}_2}$ ) and also  $\alpha_{\text{CO}} = 4.36 M_{\odot}(\text{K km s}^{-1} \text{pc}^2)^{-1}$  is assumed. Also, for galaxies taken from Bothwell et al. (2013) a typical half-light-radius of 3.0 kpc is assumed in order to estimate the surface densities. The error-bar on the top left represents a typical error on the data points. The large black circle represents the host galaxy of GRB 080207 at  $z = 2.086$  and the three other GRB hosts with detected CO emission lines are marked with orange, red, and blue large circles, assuming  $\alpha_{\text{CO}} = 4.36 M_{\odot}(\text{K km s}^{-1} \text{pc}^2)^{-1}$  for all four host galaxies. Note that this assumption is likely to result in underestimating the molecular gas masses of the GRB hosts with sub-solar metallicities and consequently providing lower limits for the surface-densities of their molecular gas mass (see Section 4 for details).

similar to those of the mentioned individual clump in the  $z \sim 2$  clumpy SFG presented in Newman et al. (2012a) where the presence of a super-wind is proposed.

Given the large separation of  $\sim 390 \text{ km s}^{-1}$  between the narrow and the broad components in our fit, it is also conceivable that the broad emission in  $\text{H}\alpha$  is associated with a companion galaxy interacting with the GRB host. This is consistent with the irregular morphology of the galaxy (Fig. 2) which suggests the possibility of an interacting system (Svensson et al. 2012). However, considering the large velocity width of the broad component, its associated gas is unlikely to be gravitationally bound and is plausibly originating from an outflowing gas either in the GRB host or in an interacting companion. Spatially resolved follow up observations are required in order to find out the nature of this broad emission.

#### 4 DISCUSSION ON THE MOLECULAR GAS CONTENT OF GRB HOSTS

It has been suggested that GRB host galaxies are deficient in molecular gas. This is mainly based on the measured molecular gas content of three GRB host galaxies: GRB 980425 at  $z = 0.0087$ , GRB 080517 at  $z = 0.089$ , and GRB 051022 at  $z = 0.81$ .

For the host galaxy of GRB 980425, Michałowski et al. (2016) report the molecular gas mass to be a factor of 3-7 less than expected from the atomic gas content and stellar mass of the galaxy. However, their comparison relies on the empirical relations of large spiral galaxies with measured atomic and molecular gas masses. This is while GRB 980425 host has a stellar mass

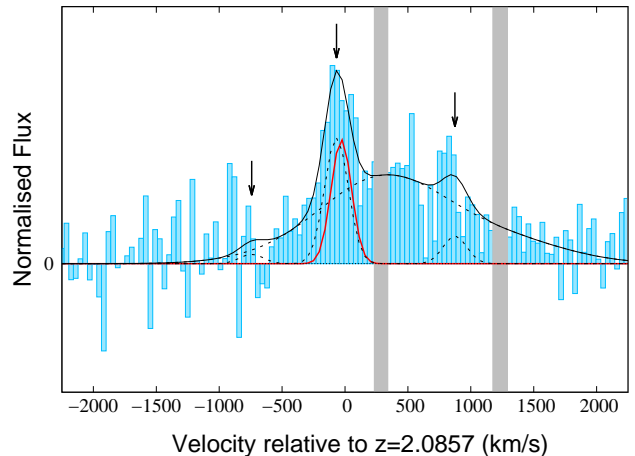


**Figure 5.** The  $\text{H}\alpha$  and  $\text{NII}$  emission lines from the host galaxy of GRB 080207. The best-fitting 2-component model is shown with the black-solid line. The narrow and broad components are marked with black-dotted lines. The best-fitting Gaussian to the  $\text{CO}(3-2)$  emission line is shown with the solid red line, scaled in y-axis such that its peak matches that of the narrow component of the  $\text{H}\alpha$  line. The vertical gray regions present the wavelengths with contamination from the sky-lines. The three arrows mark the peaks of the narrow  $\text{H}\alpha$ ,  $[\text{NII}]\lambda 6548$ , and  $[\text{NII}]\lambda 6584$  lines.

of  $M_* = 10^{8.6} M_{\odot}$  (Michałowski et al. 2014) which is typical of dwarf galaxies. If we compare its molecular gas mass with those of local dwarf galaxies with similar stellar masses, we find that

the host galaxy is quite normal in its molecular gas content (see Fig. 5 in Grossi et al. 2016, and note that the  $M_{\text{mol-gas}}/M_*$  ratio flattens at low stellar masses). This GRB host clearly follows the  $L_{\text{CO}(2-1)} - \text{SFR}$  relation. Using its half-light radius  $R_{0.5} = 4$  kpc (Michałowski et al. 2014) and assuming a Galactic  $\alpha_{\text{CO}}$ , it also appears to follow the K-S relation (see the right panel of Fig. 4). Note that  $\alpha_{\text{CO}} \gtrsim 10.0$  (Schrubba et al. 2012; Genzel et al. 2012) is a more appropriate assumption for this galaxy given its low metallicity of  $Z = 0.3Z_{\odot}$  (Christensen et al. 2008). This will shift the position of this host towards even larger molecular gas surface densities in the right panel of Fig. 4. We should mention that this GRB host also obeys the  $\Sigma_{\text{total-gas}} - \Sigma_{\text{SFR}}$  (Kennicutt 1998) when considering its atomic+molecular gas mass (Arabsalmani et al. 2015b; Michałowski et al. 2015).

A similar case is applicable to the host galaxy of GRB 051022 with a metallicity of  $Z = 0.6Z_{\odot}$ . This host (Hatsukade et al. 2014) is shown in the  $\Sigma_{\text{mol-gas}} - \Sigma_{\text{SFR}}$  plane in the right panel of Fig. 4 with a Galactic  $\alpha_{\text{CO}}$  and assuming  $R_{0.5} = 2.5$  kpc (based on the relation between  $R_{0.5}$  and stellar mass from Shibuya et al. 2015). A metallicity-dependent  $\alpha_{\text{CO}}$  for this galaxy will shift its position towards larger molecular gas surface densities on the K-S plane. It will also lead to a molecular gas fraction consistent with those of SFGs with similar specific SFR values and redshifts (see Fig. 6 of Tacconi et al. 2013).

For the host galaxy of GRB 080517, Stanway et al. (2015b) assumed a Galactic  $\alpha_{\text{CO}}$  and found the galaxy to have a molecular gas fraction similar to those of local SFGs, but with shorter molecular gas depletion time compared to the average value for the local SFGs with similar stellar masses. This host too is shown on the right panel of Fig. 4 on the  $\Sigma_{\text{mol-gas}} - \Sigma_{\text{SFR}}$  plane with  $R_{0.5} = 2.7$  taken from Stanway et al. (2015a). Note that there is no metallicity measurement available for this host. Given its stellar mass of  $M_* = 10^{9.6} M_{\odot}$  (Stanway et al. 2015a) this host is expected to have a sub-solar metallicity (see Arabsalmani et al. 2018, for the mass-metallicity relation of GRB host galaxies) and hence assuming a Galactic  $\alpha_{\text{CO}}$  should provide a lower limit for its molecular gas mass.

We emphasize that when investigating the issue of molecular gas deficiency one should be cautious of the typical low metallicities of GRB hosts and hence take into account the correct assumptions about the CO-to-molecular-gas conversion factor. In addition, any comparison should be done with similar galaxies in terms of overall properties.

For GRB 080207 host galaxy, as discussed in Section 3.2, its molecular gas properties are typical of SFGs with similar stellar masses and redshifts. Increasing the sample size of GRB host galaxies with measured molecular gas mass is required in order to draw any conclusion on the content of molecular gas in GRB hosts compared to the general SFG population.

## 5 SUMMARY

In this paper we present the molecular gas properties of GRB 080207 host galaxy at  $z = 2.086$ . This is the fourth GRB host with molecular gas detected in emission, and the first beyond redshift 1. We show that the host galaxy of GRB 080207 has molecular gas properties similar to those of the SFG population at similar redshifts. We also discuss that the reported molecular gas deficiency in other three GRB hosts with detected CO emission lines may not be real. We emphasize that when investigating the issue of molecular gas deficiency one should be cautious to compare similar galaxies

in terms of overall properties, and to take into account the correct assumptions about the CO-to-molecular-gas conversion factor for the galaxy in question.

We also compare the kinematics of the CO(3-2) emission line with that of the H $\alpha$  emission line from the host galaxy of GRB 080207. We find the H $\alpha$  emission to have contribution from two separate components, a narrow and a broad one. The narrow component appears to match well with the CO(3-2) emission line in velocity space. We speculate that the broad component is associated with a strong outflowing gas in the GRB host or in a companion galaxy interacting with the host.

## ACKNOWLEDGMENTS

We would like to thank Diego Gotz and Giulia Migliori for their support and help, and Attila Kovacs for valuable help with CRUSH software in data reduction. M. A. would like to thank Sambit Roychowdhury, Bernd Husemann, Daniel Perley, and Johan Fynbo for valuable discussions. We acknowledge the financial support from: UnivEarthS Labex program at Sorbonne Paris Cité (ANR-10-LABX-0023 and ANR-11-IDEX-0005-02) for M.A., French National Research Agency (ANR) under contract ANR-16-CE31-0003 BEaPro for S.D.V., the MINECO under the 2014 Ramón y Cajal program MINECO RYC-2014-15686 for H.D., NOVA and NWO-FAPESP grant for advanced instrumentation in astronomy for J.J., the European Union Horizon 2020 research and innovation programme under the Marie Skłodowska-Curie grant agreement No 664931 for C.F.. This work is based on observations carried out under project number w0c9/2013 with the IRAM NOEMA Interferometer. IRAM is supported by INSU/CNRS (France), MPG (Germany) and IGN (Spain).

## REFERENCES

- Acker A., Köppen J., Samland M., Stenholm B., 1989, *The Messenger*, **58**, 44
- Arabsalmani M., Møller P., Fynbo J. P. U., Christensen L., Freudling W., Savaglio S., Zafar T., 2015a, *MNRAS*, **446**, 990
- Arabsalmani M., Roychowdhury S., Zwaan M. A., Kanekar N., Michałowski M. J., 2015b, *MNRAS*, **454**, L51
- Arabsalmani M., et al., 2018, *MNRAS*, **473**, 3312
- Arnouts S., Cristiani S., Moscardini L., Matarrese S., Lucchin F., Fontana A., Giallongo E., 1999, *MNRAS*, **310**, 540
- Bothwell M. S., et al., 2013, *MNRAS*, **429**, 3047
- Bruzual G., Charlot S., 2003, *MNRAS*, **344**, 1000
- Calzetti D., Armus L., Bohlin R. C., Kinney A. L., Koornneef J., Storchi-Bergmann T., 2000, *ApJ*, **533**, 682
- Carilli C. L., Walter F., 2013, *ARA&A*, **51**, 105
- Chabrier G., 2003, *PASP*, **115**, 763
- Chary R., Elbaz D., 2001, *ApJ*, **556**, 562
- Christensen L., Vreeswijk P. M., Sollerman J., Thöne C. C., Le Floc’h E., Wiersema K., 2008, *A&A*, **490**, 45
- Combes F., García-Burillo S., Braine J., Schinnerer E., Walter F., Colina L., 2013, *A&A*, **550**, A41
- D’Elia V., et al., 2014, *A&A*, **564**, A38
- Daddi E., et al., 2010, *ApJ*, **713**, 686
- Daddi E., et al., 2015, *A&A*, **577**, A46
- Dannerbauer H., Daddi E., Riechers D. A., Walter F., Carilli C. L., Dickinson M., Elbaz D., Morrison G. E., 2009, *ApJ*, **698**, L178
- Elbaz D., et al., 2011, *A&A*, **533**, A119
- Feruglio C., et al., 2015, *A&A*, **583**, A99
- Förster Schreiber N. M., et al., 2014, *ApJ*, **787**, 38
- Friis M., et al., 2015, *MNRAS*, **451**, 167

- Fruchter A. S., et al., 2006, *Nature*, 441, 463
- Fynbo J. P. U., et al., 2009, *ApJS*, 185, 526
- Genzel R., et al., 2010, *MNRAS*, 407, 2091
- Genzel R., et al., 2012, *ApJ*, 746, 69
- Genzel R., et al., 2014, *ApJ*, 796, 7
- Grossi M., et al., 2016, *A&A*, 590, A27
- Hatsukade B., Ohta K., Endo A., Nakanishi K., Tamura Y., Hashimoto T., Kohnno K., 2014, *Nature*, 510, 247
- Hunt L., Palazzi E., Rossi A., Savaglio S., Cresci G., Klose S., Michałowski M., Pian E., 2011, *ApJ*, 736, L36
- Hunt L. K., et al., 2014, *A&A*, 565, A112
- Jakobsson P., et al., 2006, *A&A*, 460, L13
- Kelly P. L., Filippenko A. V., Modjaz M., Kocevski D., 2014, *ApJ*, 789, 23
- Kennicutt Jr. R. C., 1998, *ApJ*, 498, 541
- Kennicutt R. C., Evans N. J., 2012, *ARA&A*, 50, 531
- Kovács A., 2008, in *Millimeter and Submillimeter Detectors and Instrumentation for Astronomy IV*. p. 70201S ([arXiv:0805.3928](https://arxiv.org/abs/0805.3928)), [doi:10.1117/12.790276](https://doi.org/10.1117/12.790276)
- Krühler T., et al., 2012, *ApJ*, 758, 46
- Krühler T., et al., 2013, *A&A*, 557, A18
- Krühler T., et al., 2015, *A&A*, 581, A125
- Lagos C. d. P., Lacey C. G., Baugh C. M., 2013, *MNRAS*, 436, 1787
- Le Flocc'h E., et al., 2003, *A&A*, 400, 499
- Ledoux C., Vreeswijk P. M., Smette A., Fox A. J., Petitjean P., Ellison S. L., Fynbo J. P. U., Savaglio S., 2009, *A&A*, 506, 661
- Michałowski M. J., et al., 2014, *A&A*, 562, A70
- Michałowski M. J., et al., 2015, *A&A*, 582, A78
- Michałowski M. J., et al., 2016, *A&A*, 595, A72
- Newman S. F., et al., 2012a, *ApJ*, 752, 111
- Newman S. F., et al., 2012b, *ApJ*, 761, 43
- Noterdaeme P., Ledoux C., Petitjean P., Srianand R., 2008, *A&A*, 481, 327
- Obreschkow D., Heywood I., Klöckner H.-R., Rawlings S., 2009, *ApJ*, 702, 1321
- Perley D. A., et al., 2013, *ApJ*, 778, 128
- Perley D. A., Hjorth J., Tanvir N. R., Perley R. A., 2017a, *MNRAS*, 465, 970
- Perley D. A., et al., 2017b, *MNRAS*, 465, L89
- Prochaska J. X., Chen H.-W., Dessauges-Zavadsky M., Bloom J. S., 2007, *ApJ*, 666, 267
- Prochaska J. X., et al., 2009, *ApJ*, 691, L27
- Rodighiero G., et al., 2011, *ApJ*, 739, L40
- Rossi A., et al., 2012, *A&A*, 545, A77
- Savaglio S., Glazebrook K., Le Borgne D., 2009, *ApJ*, 691, 182
- Schruba A., et al., 2012, *AJ*, 143, 138
- Shibuya T., Ouchi M., Harikane Y., 2015, *ApJS*, 219, 15
- Siringo G., et al., 2009, *A&A*, 497, 945
- Sokolov V. V., et al., 2001, *A&A*, 372, 438
- Solomon P. M., Downes D., Radford S. J. E., Barrett J. W., 1997, *ApJ*, 478, 144
- Stanway E. R., Levan A. J., Tanvir N., Wiersema K., van der Horst A., Mundell C. G., Guidorzi C., 2015a, *MNRAS*, 446, 3911
- Stanway E. R., Levan A. J., Tanvir N. R., Wiersema K., van der Laan T. P. R., 2015b, *ApJ*, 798, L7
- Storey P. J., Zeippen C. J., 2000, *MNRAS*, 312, 813
- Svensson K. M., et al., 2012, *MNRAS*, 421, 25
- Tacconi L. J., et al., 2010, *Nature*, 463, 781
- Tacconi L. J., et al., 2013, *ApJ*, 768, 74
- Wilson C. D., et al., 2012, *MNRAS*, 424, 3050